

Cite this: *RSC Adv.*, 2017, 7, 22243

Received 9th March 2017

Accepted 13th April 2017

DOI: 10.1039/c7ra02870a

rsc.li/rsc-advances

# Aromatic cage-like B<sub>46</sub>: existence of the largest decagonal holes in stable atomic clusters†

Truong Ba Tai \*<sup>ab</sup> and Minh Tho Nguyen <sup>c</sup>

The most stable form of B<sub>46</sub> has a cage-like structure containing two hexagonal, two heptagonal and two decagonal holes. The intriguing presence of decagonal holes is a remarkable breakthrough since such large holes have never been found before for atomic clusters. This finding not only provides more insights into the growth motif of large-sized boron clusters, but also presents a new family of cage-like boron clusters containing large B<sub>N</sub> holes with N = 6–10.

## Introduction

Exhibiting a wide range and an unpredictability of structural characteristics, boron clusters are of great interest to theoretical and experimental scientists.<sup>1–6</sup> The early studies showed that small boron clusters at neutral state B<sub>n</sub> (n = 2–19) have planar or quasi-planar structures containing basic triangular units.<sup>1–3</sup> At larger sizes, they exhibit more complex geometries, including convex structures or tubular shapes containing either two or three N-membered rings connected together in antiprism bonding motif and quasi-planar geometries containing N-membered holes (N = 5–8).<sup>7,8</sup> Interestingly, while their cationic state prefers the double-ring shapes at smaller sizes,<sup>5,9</sup> anionic species B<sub>n</sub><sup>–</sup> remain the quasi-planar geometrical structures up to B<sub>40</sub><sup>–</sup>.<sup>10</sup>

Stimulated by the discovery of carbon fullerene C<sub>60</sub> (ref. 11) and its unique properties, the search for cage-like boron clusters has been greatly attractive over the last decade. The buckyball B<sub>80</sub>, an isoelectronic species of the fullerene C<sub>60</sub>, was proposed in 2007 (ref. 12) and has received much attention,<sup>13,14</sup> although recent theoretical studies reported that core-shell structures are more favourable in energy.<sup>15</sup> Recently, the B<sub>40</sub> cluster was found as a stable all-boron fullerene containing four heptagonal holes and two hexagonal holes.<sup>10,16,17</sup> In the combined experimental and theoretical study, Wang *et al.*<sup>10</sup> reported that this caged structure was somewhat less stable than a quasi-planar structure containing two hexagonal holes and both of them were identified in the photoelectron spectrum. These findings marked a breakthrough in the discovery of boron clusters since the anion B<sub>40</sub><sup>–</sup> is the first cage-like boron cluster which was observed in experiment. A few cage-like

systems such as B<sub>38</sub>,<sup>18</sup> B<sub>39</sub><sup>–</sup>, B<sub>41</sub><sup>+</sup> and B<sub>42</sub><sup>2+</sup> were subsequently reported.<sup>19</sup> A common structural feature of these systems is that they are composed of the hexagonal and heptagonal holes. Smaller cage-like structures B<sub>14</sub>, B<sub>28</sub><sup>0/–</sup> and B<sub>29</sub><sup>–</sup> were also reported as smallest boron cages which were almost degenerate with the planar structures.<sup>20,21</sup> More recently, we found that the B<sub>42</sub><sup>+</sup> and B<sub>44</sub> also have, for their lowest-energy form, cage-like structures which contain eight- and nine-membered holes, respectively (Fig. 1).<sup>22</sup> The neutral cage-like B<sub>42</sub> is nearly degenerate with a triple ring tube of 14-atom strings. The presence of such large holes is intriguing since they have been found for the first time in atomic clusters, and has stimulated us to further explore larger sized species B<sub>n</sub> to find out elements for the answer to the question as to whether boron clusters with larger holes exist.

In the present work, we report on the existence of the boron cluster B<sub>46</sub> which exhibits a cage-like structure containing two hexagonal, two heptagonal and two decagonal (ten-membered) holes. The presence of decagonal holes has never been found before in atomic clusters, of either main group elements or transition metals. The present work does not only provide more

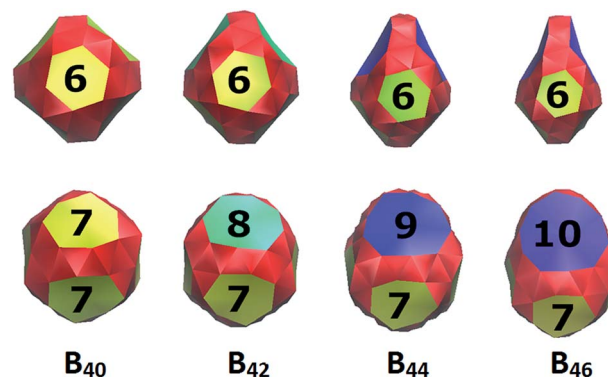


Fig. 1 Shape of the most stable structures of B<sub>n</sub> with n = 40, 42, 44 and 46.

<sup>a</sup>Computational Chemistry Research Group, Ton Duc Thang University, Ho Chi Minh City, Vietnam. E-mail: truongbatai@tdt.edu.vn

<sup>b</sup>Faculty of Applied Sciences, Ton Duc Thang University, Ho Chi Minh City, Vietnam

<sup>c</sup>Department of Chemistry, KU Leuven, Leuven City, Belgium

† Electronic supplementary information (ESI) available. See DOI: 10.1039/c7ra02870a

insight into the growth motif of boron clusters, but it also shows a new family of cage-like boron clusters containing large hole  $B_N$  with  $N = 6$ –10 (Fig. 1).

## Computational methods

Extensive structural searches for  $B_{46}$  were carried out by using stochastic random searching procedures,<sup>23</sup> and manual structural construction based on the known structures of smaller sized boron clusters<sup>17–19,22</sup> by using the PBE0 functional<sup>24</sup> in conjunction with small basis set 3-21G.<sup>25</sup> Low-lying isomers  $B_{46}$  with relative energy of 0.0–5.0 eV obtained from initial geometry optimizations at the PBE0/3-21G were fully re-optimized at the higher level PBE0/6-311+G(d).<sup>26</sup> To identify a true global minimum, single-point electronic energies of a few lowest-lying  $B_{46}$  isomers were subsequently calculated using the couple-cluster theory CCSD(T)/6-31G(d) method<sup>27</sup> at their PBE0/6-311+G(d) optimized geometries. These computational methods were used to effectively establish the energy landscape of boron clusters in the literature.<sup>3,4,7–9,22</sup> All calculations were performed using the Gaussian 09 (ref. 28) and Molpro 2009 packages.<sup>29</sup>

## Results and discussion

Identification of the global minimum for  $B_{46}$  was carried out using the DFT and CCSD(T) methods. The optimized geometries and relative energies (eV) of a few lowest-lying  $B_{46}$  isomers are depicted in Fig. 2, while those of less stable isomers are shown in Fig. S1 of the (ESI†) file. At the CCSD(T)/6-31G(d)//PBE0/6-311+G(d) level, our computed results show that structure **I** ( $C_{2v}$ ,  $^1A_1$ ) which contains two hexagonal, two heptagonal and two decagonal holes is the most stable form. This structure is composed of 54 triangular units and six polygonal holes. The latter includes two decagonal  $B_{10}$ , two heptagonal  $B_7$  and two hexagonal  $B_6$  holes. This isomer can be constructed by replacing

two neighbored heptagonal  $B_7$  holes of the  $B_{40}$  fullerene by two decagonal  $B_{10}$  holes and following the Euler's rule for a polyhedron:  $E(104 \text{ edges}) = F(54 \text{ triangular} + 2 \text{ hexagonal} + 2 \text{ heptagonal} + 2 \text{ decagonal faces}) + V(46 \text{ vertices}) - 2$ .

Although a quasi-planar structure **II** ( $C_{2v}$ ,  $^1A_1$ ) which contains one hexagonal hole is more stable at the PBE0/6-311+G(d) level, it is 0.53 eV less stable than **I** at the CCSD(T)/6-31G(d). These calculated results are consistent with the early reports that the PBE0 tends to overestimate the cohesive energy of the quasi-planar or planar structures.<sup>9,30</sup> The next isomers exhibit different structural characteristics, including a quasi-planar structure **III** ( $C_1$ ,  $^1A_1$ ), a tubular form **IV** ( $C_s$ ,  $^1A'$ ) and cage-like structures **V** ( $C_1$ ,  $^1A$ ) and **VI** ( $C_1$ ,  $^1A$ ), with relative energies of at least 0.72 eV at the CCSD(T)/6-31G(d) level. The structure **III** is also quasi-planar structure containing two hexagonal hole, while the structure **IV** is tubular form which is composed of two fifteen-membered rings and one sixteen-membered ring.

As shown in Fig. 1, the clusters  $B_{40}$ ,  $B_{42}$ ,  $B_{44}$  and  $B_{46}$  have similar geometries in which two neighbored  $B_7$  holes of  $B_{40}$  were replaced by two  $B_8$ ,  $B_9$  and  $B_{10}$  holes to form the  $B_{42}$ ,  $B_{44}$  and  $B_{46}$ , respectively. We expect that these large-sized holes play as stable units in the building up of larger boron clusters.

To gain more understanding about the high stability of the isomer **I**, we performed molecular dynamics (MD) simulation for this system by using the CP2K programs.<sup>31</sup> The simulation was carried out at temperature of 500 K during a time of 30 ps using the PBE functional in conjunction with the 6-31G(d) basis set. RMSD values were calculated using the VMD code<sup>32</sup> and their plots are depicted in Fig. 3 together with the movie of simulation trajectory at 500 K (ESI†). During the BO-MD simulation at 500 K, the isomer **I** retains its connectivity pattern and cage-like shape with two decagonal holes. The root mean square deviation (RMSD) varies in range of 0.11 to 0.26 Å. The high stability of decagonal holes is of fundamental characteristic and gives us more understanding about the growth mechanism of boron clusters.

The characteristics of electron delocalization and aromaticity of boron clusters have attracted much attention since they provide us with better understanding about their stability. The

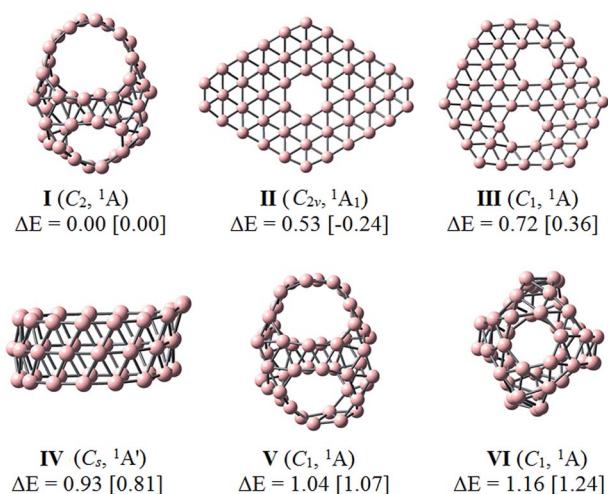


Fig. 2 Optimized geometries and relative energies (eV) of the lowest-lying isomers  $B_{46}$  obtained at the CCSD(T)/6-31G(d)//PBE0/6-311+G(d) level of theory (in square brackets are PBE0/6-311+G(d) values).

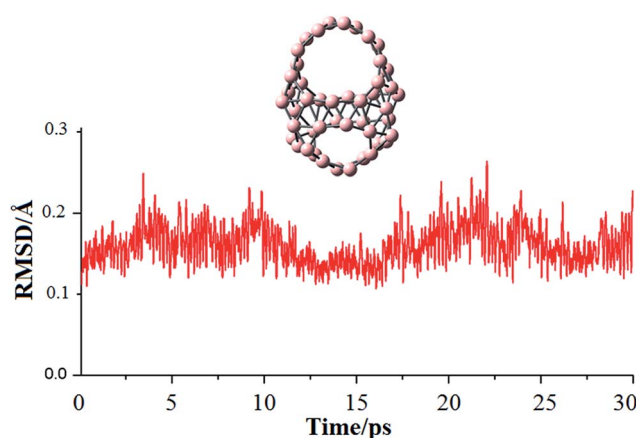


Fig. 3 Born–Oppenheimer molecular simulation of the lowest isomer  $B_{46}$  at 500 K.



aromatic feature of  $B_{46}$  is first evaluated using the nucleus independent chemical shift (NICS)<sup>33</sup> which is one common criterion to evaluate the molecular aromaticity. Our NICS calculations at the central position of structure **I** point out that this cage is highly aromatic with a large negative NICS value of  $-26$  ppm. This value is comparable to the NICS values obtained earlier for boron cages, *e.g.*  $-38$  ppm for  $B_{39}^-$ ,<sup>19a</sup>  $-42$  ppm for  $B_{40}$  (ref. 10) and  $-21$  ppm for  $B_{44}$ .<sup>22a</sup> In the previous report, using the profiles of the  $z$ -component of the induced magnetic field ( $B_z^{\text{ind}}$ ), Merino *et al.*<sup>17a</sup> showed that the intensity of  $B_z^{\text{ind}}$  in  $B_{40}$  diminishes gradually along the center to the surface of cage  $B_{40}$ . Based on the computed  $B_z^{\text{ind}}$  profiles, these authors also indicated that there is strong delocalization in  $\sigma$ -electron systems of both 6- and 7-membered rings. While the  $\pi$ -electron system of the 6-membered rings presents strong delocalization, the  $\pi$ -electron delocalization of the 7-membered rings is much less.

To have more insight into the high stability and aromaticity of **I**, we performed a topological analysis of the electron localization function (ELF).<sup>34</sup> This approach does not only give us a general view of bonding pattern and electron distribution, but also allows the aromatic feature of the systems to be examined on the basis of their bifurcation values of the  $ELF_\sigma$  and  $ELF_\pi$  components.<sup>7,22,35</sup> Accordingly, each total ELF map can be partitioned in terms of separate  $ELF_\sigma$  and  $ELF_\pi$  components that arise from the contributions of  $\sigma$  and  $\pi$  electrons, respectively. An aromatic system possesses a high ELF bifurcation value, whereas the corresponding bifurcation value is low in an anti-aromatic system. The ELF analysis was carried out by using the Dgrid-4.6 package.<sup>36</sup>

Our analysis of canonical molecular orbitals (CMOs) for **I** shows that this species contains a total of 69 valence MOs which are separated into 55  $\sigma$ -MOs and 14  $\pi$ -MOs. The  $ELF_\pi$  and  $ELF_\sigma$  plots depicted in Fig. 4 emphasize an excellent electron delocalization for both  $\sigma$  and  $\pi$  electron systems of cage-like structure **I**. At the value of  $ELF_\sigma = 0.85$ , the isosurface of the  $ELF_\sigma$  is separated into 54 basins that determine the chemical bonding of 54 triangular units. The isosurface of  $ELF_\pi$  is separated at the bifurcation value of  $ELF_\pi = 0.70$  which consequently indicates a  $\pi$  electron delocalization over the whole system. In general, such an electron distribution with high bifurcation values gives rise to two highly delocalized  $\sigma$  and  $\pi$  bonding systems, which make the isomer **I** aromatic and thereby highly thermodynamically stable.

To probe a better understanding about the chemical bonding characteristic of the  $B_{46}$ , the further analysis was carried out for the most stable isomer **I** by using adaptive natural density partitioning (AdNDP) method.<sup>37</sup> This approach was effectively used to analyze the chemical bonds of boron clusters in the early reports.<sup>4c,10,19</sup> As shown in Fig. 5, 69 valence electron pairs of the isomer **I** are almost delocalized over structure and form 55  $\sigma$ -bonds and 14  $\pi$ -bonds. First set includes 46(3c-2e)  $\sigma$ -bonds (Fig. 5a) and 8(6c-2e)  $\sigma$ -bonds (Fig. 5b) which distribute on 54 triangle units. The remaining (6c-2e)  $\sigma$ -bond is located at top of structure (Fig. 5b) that supports for high stability of two ten-membered rings.

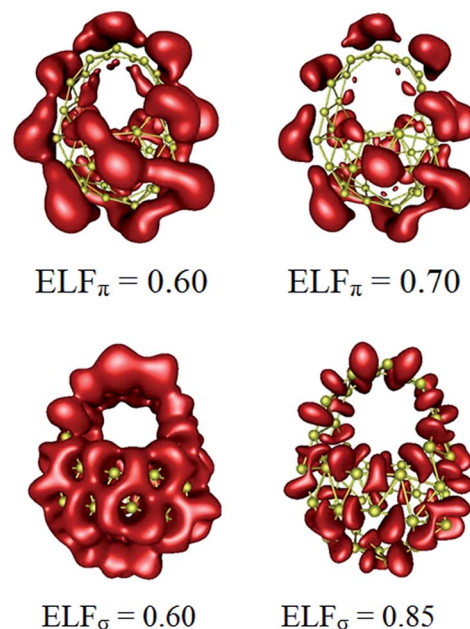


Fig. 4 Plots of  $ELF_\pi$  (up) and  $ELF_\sigma$  (down) of the cage-like structure **I**.

Interestingly, second set includes 4 (5c-2e)  $\pi$ -bonds and 10 (6c-2e)  $\pi$ -bonds that are delocalized over planar boron double chains (BDCs) of the  $B_{46}$  (Fig. 5c). This delocalized  $\sigma$  and  $\pi$ -bonding pattern agrees well with our above ELF analysis and strongly supports for high stability of the  $B_{46}$  **I**.

The vibrational spectrum is interesting and helpful since it allows us to identify structural characteristics. To assist future experimental studies, simulations of infrared (IR) spectra of two stable lowest-lying isomers **I** and **II** obtained at the PBE0/6-311+G(d) level are shown in Fig. 6. While the IR spectrum of the planar structure **II** exhibits many intensive peaks in a large range of  $500\text{--}1400\text{ cm}^{-1}$ , the spectrum of **I** is more concentrated in the range of  $1200\text{--}1400\text{ cm}^{-1}$  and characterized by much less intensive peaks at low frequencies. For isomer **I**, seven major peaks appear at  $381, 621, 799, 1029, 1232, 1293$  and  $1355\text{ cm}^{-1}$  which correspond to the intense peaks centered of  $380, 713$  and  $1274\text{ cm}^{-1}$  of the cage  $B_{40}$ ,<sup>17</sup> and the peaks of  $390, 776, 1005, 1231, 1275\text{ cm}^{-1}$  of the cage-like  $B_{44}$ .<sup>22</sup>

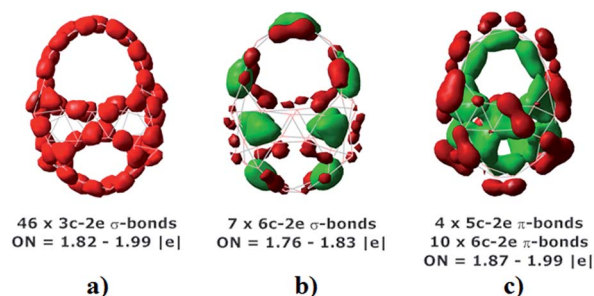


Fig. 5 The AdNDP bonding pattern of isomer **I** with occupation number (ON).





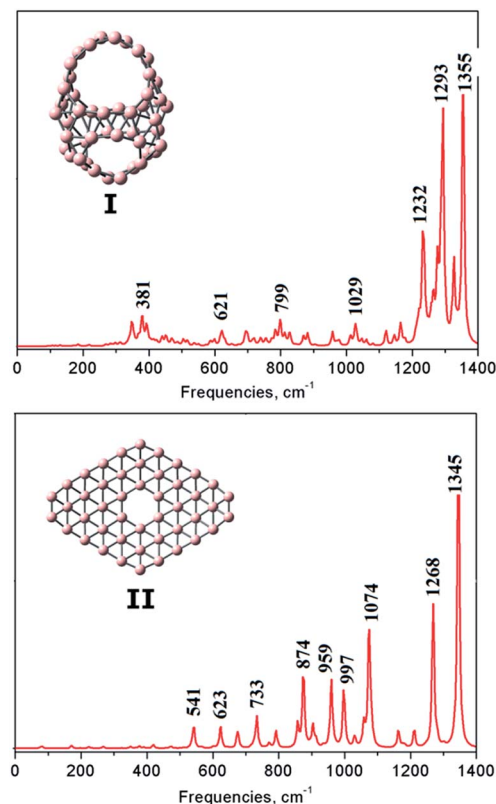


Fig. 6 Simulated infrared spectra of the lowest-lying  $B_{46}$  isomers.

## Conclusions

In conclusion, we performed a theoretical study on the  $B_{46}$  cluster by using DFT and CCSD(T) methods, and found that the most stable form of  $B_{46}$  is the cage-like structure I containing two decagonal, two heptagonal and two hexagonal holes. The structure I is composed of two delocalized  $\sigma$  and  $\pi$  bonding systems that rationalize its high stability. BO-MD simulations at 500 K showed that the  $B_{46}$  is both thermodynamically and kinetically stable. The analysis of chemical bonding characteristics showed that the  $B_{46}$  contains two delocalization  $\sigma$  and  $\pi$  electron systems that supports for its enhanced stability. The presence of decagonal holes again marks a breakthrough since it has been never found before in elemental clusters. The present work does not only provide more insight into the growth motif of boron clusters, but it also emphasizes a new family of cage-like boron clusters containing large holes  $B_N$  with  $N = 6-10$ .

## Acknowledgements

We are indebted to the KU Leuven Research Council (GOA program) and Vlaams Supercomputer Centrum (VSC).

## Notes and references

- (a) I. Boustani, Z. Zhu and D. Tomanek, *Phys. Rev. B: Condens. Matter Mater. Phys.*, 2011, **83**, 193405; (b) I. Boustani, *Chem. Modell.*, 2011, **8**, 1; (c) S. Chacko,

D. G. Kanhere and I. Boustani, *Phys. Rev. B: Condens. Matter Mater. Phys.*, 2003, **68**, 035414.

- (a) W. L. Li, Y. F. Zhao, H. S. Hu, J. Li and L. S. Wang, *Angew. Chem., Int. Ed.*, 2014, **53**, 5540; (b) C. Romanescu, D. J. Harding, A. Fielicke and L. S. Wang, *J. Chem. Phys.*, 2012, **137**, 014317; (c) A. N. Alexandrova, A. I. Boldyrev, H.-J. Zhai and L.-S. Wang, *Coord. Chem. Rev.*, 2006, **250**, 2811; (d) Z. A. Piazza, I. A. Popov, W.-L. Li, R. Pal, X. C. Cheng, A. I. Boldyrev and L. S. Wang, *J. Chem. Phys.*, 2014, **141**, 034303; (e) I. A. Popov, Z. A. Piazza, W. L. Li, L. S. Wang and A. I. Boldyrev, *J. Chem. Phys.*, 2013, **139**, 144307; (f) W. Huang, A. P. Sergeeva, H. J. Zhai, B. B. Averkiev, L. S. Wang and A. I. Boldyrev, *Nat. Chem.*, 2010, **2**, 202.
- (a) A. G. Arvanitidis, T. B. Tai, M. T. Nguyen and A. Ceulemans, *Phys. Chem. Chem. Phys.*, 2014, **16**, 18311; (b) T. B. Tai, A. Ceulemans and M. T. Nguyen, *Chem.-Eur. J.*, 2012, **18**, 4510; (c) H. T. Pham, L. V. Duong, B. Q. Pham and M. T. Nguyen, *Chem. Phys. Lett.*, 2013, **557**, 32; (d) T. B. Tai, D. J. Grant, M. T. Nguyen and D. A. Dixon, *J. Phys. Chem. A*, 2010, **114**, 994; (e) T. B. Tai, N. M. Tam and M. T. Nguyen, *Chem. Phys. Lett.*, 2012, **530**, 71.
- (a) J. O. C. Jimenez-Halla, R. Islas, T. Heine and G. Merino, *Angew. Chem., Int. Ed.*, 2010, **49**, 5668; (b) D. Moreno, S. Pan, L. Liu-Zeonjuk, R. Islas, E. Osorio, G. M. Guajardo, P. K. Chattaraj, T. Heine and G. Merino, *Chem. Commun.*, 2014, **50**, 8140; (c) F. Cervantes-Navarro, G. Martinez-Guajardo, E. Osorio, D. Moreno, W. Tiznado, R. Islas, K. J. Donald and G. Merino, *Chem. Commun.*, 2014, **50**, 10680; (d) G. Martinez-Guajardo, A. P. Sergeeva, A. I. Boldyrev, T. Heine, J. M. Ugalde and G. Merino, *Chem. Commun.*, 2011, **47**, 6242; (e) S. Jalife, L. Liu, S. Pan, J. L. Cabellos, E. Osorio, C. Lu, T. Heine, K. J. Donald and G. Merino, *Nanoscale*, 2016, **8**, 17639.
- E. Oger, N. R. M. Crawford, R. Kelting, P. Weis, M. M. Kappes and R. Ahlrichs, *Angew. Chem., Int. Ed.*, 2007, **46**, 8503.
- (a) S. Li, Z. Zhang, Z. Long, G. Sun and S. Qin, *Sci. Rep.*, 2016, **6**, 1; (b) A. B. Rahane and V. Kumar, *Nanoscale*, 2015, **7**, 4055.
- (a) T. B. Tai, L. V. Duong, H. T. Pham, D. T. T. Mai and M. T. Nguyen, *Chem. Commun.*, 2014, **50**, 1558; (b) T. B. Tai and M. T. Nguyen, *Chem. Commun.*, 2015, **51**, 7677; (c) T. B. Tai and M. T. Nguyen, *Phys. Chem. Chem. Phys.*, 2015, **17**, 13672.
- (a) Z. A. Piazza, H.-S. Hu, W.-L. Li, Y.-F. Zhao, J. Li and L.-S. Wang, *Nat. Commun.*, 2014, **5**, 31; (b) W. L. Li, Q. Chen, W. J. Tian, H. Bai, Y. F. Zhao, H. S. Hu, J. Li, H. J. Zhai, S. D. Li and L. S. Wang, *J. Am. Chem. Soc.*, 2014, **126**, 12257; (c) B. Kiran, S. Bulusu, H.-J. Zhai, S. Yoo, X. C. Zeng and L. S. Wang, *Proc. Natl. Acad. Sci. U. S. A.*, 2005, **102**, 961.
- T. B. Tai, N. M. Tam and M. T. Nguyen, *Theor. Chem. Acc.*, 2012, **131**, 1241.
- H.-J. Zhai, Y.-F. Zhao, W.-L. Li, Q. Chen, H. Bai, H.-S. Hu, Z. A. Piazza, W.-J. Tian, H.-G. Lu, Y.-B. Wu, Y.-W. Mu, G.-F. Wei, Z.-P. Liu, J. Li, S.-D. Li and L.-S. Wang, *Nat. Chem.*, 2014, **6**, 727.
- H. W. Kroto, J. R. Heath, S. C. O'Brien, R. F. Curl and R. E. Smalley, *Nature*, 1985, **318**, 162.



- 12 N. G. Szewacki, A. Sadrzadeh and B. I. Yakobson, *Phys. Rev. Lett.*, 2007, **98**, 166804.
- 13 (a) A. Ceulemans, J. T. Muya, G. Gopakumar and M. T. Nguyen, *Chem. Phys. Lett.*, 2008, **461**, 226; (b) J. T. Muya, E. Lijnen, M. T. Nguyen and A. Ceulemans, *Chem. Phys. Chem.*, 2013, **14**, 346.
- 14 (a) S. De, A. Willand, M. Amsler, P. Pochet, L. Genoverse and S. Grodecke, *Phys. Rev. Lett.*, 2011, **106**, 225502; (b) Y. Li, G. Zhou, J. Li, B.-L. Gu and W. Duan, *J. Phys. Chem. C*, 2008, **112**, 19268.
- 15 H. Li, N. Shao, B. Shang, L. F. Yuan, J. L. Yang and X. C. Zeng, *Chem. Commun.*, 2010, **46**, 387.
- 16 H. T. Pham, L. V. Duong, N. M. Tam, M. P. Pham-Ho and M. T. Nguyen, *Chem. Phys. Lett.*, 2014, **608**, 295.
- 17 (a) G. Martinez-Guajardo, J. L. Cabellos, A. Diaz-Celaya, S. Pan, R. Islas, P. K. Chattaraj, T. Heine and G. Merino, *Sci. Rep.*, 2015, **5**, 11287; (b) R. He and X. C. Zeng, *Chem. Commun.*, 2015, **51**, 3185.
- 18 (a) J. Lv, Y. Wang, L. Zhu and Y. Ma, *Nanoscale*, 2014, **6**, 11692; (b) T. B. Tai and M. T. Nguyen, *Nanoscale*, 2015, **7**, 3316.
- 19 (a) Q. Chen, W. L. Li, Y. F. Zhao, S. Y. Zhang, H. S. Hu, H. Bai, H. R. Li, W. J. Tian, H. G. Lu, H. J. Zhai, S. D. Li and L. S. Wang, *ACS Nano*, 2015, **9**, 754; (b) Q. Chen, S. Y. Zhang, H. Bai, W. J. Tian, T. Gao, H. R. Li, C. Q. Miao, Y. W. Mu, H. G. Lu, H. J. Zhai and S. D. Li, *Angew. Chem., Int. Ed.*, 2015, **54**, 8160.
- 20 (a) L. Cheng, *J. Chem. Phys.*, 2012, **136**, 104301; (b) J. Zhao, X. Huang, R. Shi, H. Liu, Y. Su and R. B. King, *Nanoscale*, 2015, **7**, 15086.
- 21 (a) Y. J. Wang, Y. F. Zhao, W. L. Li, T. Jian, Q. Chen, X. R. You, T. Ou, X. Y. Zhao, H. J. Zhai, S. D. Li and L. S. Wang, *J. Chem. Phys.*, 2016, **144**, 064307; (b) H. R. Li, T. Jian, W. L. Li, C. Q. Miao, Y. J. Wang, Q. Chen, X. M. Luo, K. Wang, H. J. Zhai, S. D. Li and L. S. Wang, *Phys. Chem. Chem. Phys.*, 2016, **18**, 29147.
- 22 (a) T. B. Tai and M. T. Nguyen, *Chem. Commun.*, 2016, **52**, 1652; (b) T. B. Tai and M. T. Nguyen, *Phys. Chem. Chem. Phys.*, 2016, **18**, 11620.
- 23 T. B. Tai and M. T. Nguyen, *J. Chem. Theory Comput.*, 2011, **7**, 1119.
- 24 (a) J. P. Perdew, K. Burke and M. Ernzerhof, *Phys. Rev. Lett.*, 1996, **77**, 3865; (b) J. P. Perdew, K. Burke and M. Ernzerhof, *Phys. Rev. Lett.*, 1997, **78**, 1396; (c) J. A. Pople, *J. Chem. Phys.*, 1980, **72**, 650.
- 25 (a) J. S. Binkley, J. A. Pople and W. J. Hehre, *J. Am. Chem. Soc.*, 1980, **102**, 939; (b) M. S. Gordon, J. S. Binkley, J. A. Pople, W. J. Pietro and W. J. Hehre, *J. Am. Chem. Soc.*, 1982, **104**, 2797; (c) K. D. Dobbs and W. J. Hehre, *J. Comput. Chem.*, 1987, **8**, 861.
- 26 (a) A. D. McLean and G. S. Chandler, *J. Chem. Phys.*, 1980, **72**, 5639; (b) K. Raghavachari, J. S. Binkley, R. Seeger and J. A. Pople, *J. Chem. Phys.*, 1980, **72**, 650.
- 27 M. Rittby and R. J. Bartlett, *J. Phys. Chem.*, 1988, **92**, 3033.
- 28 M. J. Frisch, *et al.*, *Gaussian 09, Revision C.01*, Gaussian, Inc., Wallingford CT, 2009.
- 29 H. J. Werner, *et al.*, *MOLPRO 09, version 2009.1*, 2009, see, <http://www.molpro.net>.
- 30 F. Li, P. Jin, D. Jiang, L. Wang, S. B. Zhang, J. Zhao and Z. Chen, *J. Chem. Phys.*, 2012, **136**, 074302.
- 31 J. Vande Vonele, M. Krack, F. Mohamed, M. Parrinello, Y. Chassaing and J. Hutter, *Comput. Phys. Commun.*, 2005, **8**, 1314.
- 32 W. Humphrey, A. Dalke and K. Schulten, *J. Mol. Graphics*, 1996, **14**, 33.
- 33 P. V. R. Schleyer, C. Maerker, A. Dransfeld, H. Jiao and N. J. V. E. Hommes, *J. Am. Chem. Soc.*, 1996, **118**, 6317.
- 34 A. Becke and K. Edgecombe, *J. Chem. Phys.*, 1990, **92**, 5397.
- 35 J. C. Santos, W. Tzando, R. Contreras and P. Fuentealba, *J. Chem. Phys.*, 2004, **120**, 1670.
- 36 M. Kohout, Dgrid-4.6, Radebeul, 2011.
- 37 D. Y. Zubarev and A. I. Boldyrev, *Phys. Chem. Chem. Phys.*, 2008, **10**, 5207.

